Mustansiria Dental Journal MDJ

Vol.21, No.02, 12/2025

P- ISSN: 1813-8500

E- ISSN: 2618-0944

Comparative 3D Finite Element Stress Analysis of Monolithic Lithium Disilicate and Dual-Layered Endocrown Restorations

Haider Ali Ibrahim[1], and Haider Hasan Jasim[2]

[1]Department of Conservative Dentistry, College of Dentistry, Mustansiriyah University, Baghdad, Iraq, E-mail: Haider.ali94@uomustansiriyah.edu.iq.

[2]Department of Conservative Dentistry, College of Dentistry, Mustansiriyah University, Baghdad, Iraq, E-mail: denhaider5@uomustansiriyah.edu.iq, ORCID ID: https://orcid.org/0000-0003-0636-2435.

***Received** 11/01/2025* ***Accepted** in revised form 22/12/2025* ***Published** 30/12/2025*

Abstract

Aim: Endodontically treated teeth (ETT) longevity depends on the ability of restorations to distribute occlusal forces effectively and prevent structural failures. While monolithic lithium disilicate (LDS) endocrowns are widely used, their rigid nature may lead to stress concentration, increasing the risk of failure. Therefore, this study aims to evaluate and compare the stress distribution of monolithic LDS and dual-layered endocrown restorations for endodontically treated mandibular molars using 3D finite element analysis (FEA).

Method: Cone-beam computed tomography (CBCT) was used to scan a sound mandibular first molar, and the data were processed in Mimics Materialise software to create an STL file. Two models were designed in modeling software: Model A (monolithic LDS endocrown) and Model B (dual-layered endocrown with a Lava Ultimate endocore veneered with LDS). The models were meshed using 10-node tetrahedral elements and then subjected to a 600 N axial occlusal load. A stainless-steel indenter with a 6 mm rounded end was used to provide a standardized tripod occlusal contact. Von Mises (VM) criterion was used to investigate the high and low stress patterns within the restoration complex and tooth tissues.

Result: Model A exhibited higher stress concentration at the occlusal surface and cervical regions, with a maximum VM stress of (17.20 MPa) in LDS. In contrast, Model B had a reduced VM stress of (4.87 MPa) in the LDS veneering part and (4.24 MPa) in the endocore. Stress at the enamel was (16.05 MPa) in Model A, decreasing to (9.88 MPa) in Model B. Dentin stress was also lower in Model B (3.49 MPa) compared to Model A (4.37 MPa). The tooth-restoration cement layer exhibited (5.16 MPa) in Model A and (3.49 MPa) in Model B, while the cement layer between the veneering layer and endocore had a VM stress of (3.92 MPa). The flowable composite exhibited a VM stress of 1.63 MPa in Model A and 1.33 MPa in Model B.

ConclusionDual-layered endocrowns demonstrated more favorable stress distribution compared to monolithic designs, suggesting greater durability for restoring endodontically treated teeth. Experimental validation is recommended.

Keywords: Finite Element Analysis, Endocrown, Hybrid Ceramics, Lithium Disilicate, Dual Layered, Stress Distribution.

1. Introduction

Endodontically treated teeth (ETT) restoration with massive structural loss remains a significant challenge (Schestatsky et al., 2019). Although the well-known post-core-crown restoration provides acceptable outcomes, it may compromise the biomechanical resistance and elevate the risk of structural failure (Phang et al., 2020).

The improvement of adhesive dentistry, together with a shift toward minimally invasive dentistry, has established endocrown restorations as a promising restorative option for ETT (Govare & Contrepois, 2020; Sedrez-Porto et al., 2016). Endocrowns are a monolithic design that uses the pulp chamber and remaining walls for retention (Pissis, 1995). Their advantages include sealing of root canals coronally, reducing the possibility of recontamination, excellent stability, and enhanced fracture resistance (Biacchi & Basting, 2012; El-Damanhoury et al., 2015).

Lithium disilicate (LDS) material is used popularly for indirect restorations, including endocrowns, because of its acceptable mechanical features, ability to adhesion, and high esthetic (Chen et al., 2021). As the LDS material is more rigid, with a high elastic modulus, it may result in high stress accumulation in specific regions of the tooth-restoration complex rather than being distributed; in this manner, irreparable failures could happen (Tribst et al., 2018; Sedrez-Porto et al., 2020; El Ghoul et al., 2019). To provide high biomechanical behavior, materials with tooth-friendly properties close to the dental substrates need to be used (Jargalsaikhan et al., 2024; Huang et al., 2007). Although the lost enamel could be successfully replaced with LDS material, it fails to mimic the elastic behavior of dentin (Eskitaşçioğlu et al., 2020).

On the other side, more tooth-like materials have gained popularity under the name of hybrid ceramics were introduced (Awada & Nathanson, 2015; Fathy et al., 2022; Della Bona et al., 2014). One of the hybrid ceramic categories is resin nanoceramics, which are particularly noteworthy for their ability to distribute the stress and provide satisfactory mechanical values (Ural & Çağlayan, 2021; Goujat et al., 2018). However, some of the drawbacks were noticed, including their ability to discolor, low fracture resistance, and low wear resistance (Albelasy et al., 2020).

Multilayered endocrowns emerged with the purpose of overcoming these challenges. Improvement of the biomechanical behavior and the mimicry of the structure of the tooth, at least partially, was the purpose of such an approach, with the most satisfactory outcomes (Shams et al., 2022; Eskitaşçioğlu et al., 2020).

The finite element method has long been utilized in dentistry for the determination of the pattern of stresses subjected to masticatory force. The convenience of standardizing the testing environment with the proper computation of the area of maximum stress concentration makes the finite element method ideal for determining the area most susceptible to failure. Earlier FEA research has correctly revealed that the area of maximum buildup of stresses has a greater susceptibility towards fracture (Dartora et al., 2019; Zhu et al., 2017). This study, therefore, was carried out with the aim of assessing the distribution of the dual-layer endocrown design against the monolithic standard LDS endocrown design for the reconstruction of ETT through the use of FEA.

2. Materials And Methodologies

2.1. Generation of FE models

A recently extracted sound mandibular first molar was obtained under ethical authorization from the institutional ethics committee board of the College of Dentistry, Mustansiriyah University (NO: MUOPR29), and was imaged using a CBCT device (Promax 3D Classic, Planmeca Helsinki, Finland) to obtain DICOM files for 3D model creation. MIMICS software (Mimics ver.21.0; Materialise Leuven, Belgium) was used to apply a multi-step segmentation process on the DICOM file to separate the tooth structures precisely. First, the DICOM dataset was imported into the software, and an initial thresholding technique was applied to distinguish dental tissues based on Hounsfield unit (HU) values. The enamel, dentin, and pulp chamber were identified by selecting appropriate HU ranges, ensuring clear differentiation between high-density and low-density structures. This step was fine-tuned with manual mask editing; incomplete and/or oversegmented parts were changed to clean noise and other artifacts. After the segmentation process, each tooth structure was transformed into a 3D surface model by the Marching Cubes algorithm at a high-resolution mesh. Smoothing and hole-filling algorithms were applied to the model in order to rectify the inconsistent results due to CBCT artifacts. Lastly, the segmented structure was exported in STL format. Autodesk modeling software (Fusion 360, Autodesk, USA) was used to construct endocrown restorations. The prepared tooth model was sectioned 2 mm above the CEJ and provided with a butt margin, which preserved a depth of the pulp chamber at 4 mm. Cavity dimensions were standardized: mesiodistal width of 6 mm, buccolingual width of 4 mm, and an 8° internal taper on the axial walls. The root canals were filled with simulated Gutta-percha, 0.5 mm short of the root apex. To create a flat pulpal floor, a flowable composite (SDR, Dentsply Sirona, USA) was applied with a thickness of 1 mm. Additionally, the periodontal ligament was simulated as a 0.2 mm layer surrounding the root. The bone was modeled in two parts: an outer two mm-thick cortical bone shell (dense) surrounding the inner spongy cancellous bone to better replicate the natural bone structure. The initial model was duplicated into two models depending on the type of endocrown restoration used.

Model A: Monolithic LDS endocrown

The endocrown restoration was designed with a height of 4 mm, starting at the cavosurface margin to the highest point of the buccal cusps. The cement gap between the tooth surface and endocrown restoration was modeled to be 70 µm.

Model B: Dual-layered endocrown with Lava Ultimate endocore and LDS veneering layer

The endocore was designed with a height of 2 mm from the external cavosurface margin, and its margin was 1 mm short of the cavosurface margin. Subsequently, the veneering layer was designed with a thickness of 2 mm at the occlusal surface and 1 mm at the proximal walls to cover the endocore. Two 70 µm-thick cement layers were included: one between the tooth structure and the endocore (Cement 1) and the other between the endocore and the veneering crown (Cement 2). The type of resin cement was uniform for all interfaces (Variolink II Ivoclar, Vivadent, Schaan, Liechtenstein). The design parameters are shown in Figure 1.

2.2. Finite element discretization

After developing the 3D solid models, the mesh was created and optimized using FEA software (Abaqus, Dassault Systèmes, v.2023, USA). Higher-order 10-node tetrahedral elements (C3D10) were employed to model the complex geometry and stress/strain gradients with more accurate results and convergence as compared with lower-order elements. Every node had 3 degrees of freedom, which allowed for accurate simulation of stress and deformation. The models had varying amounts of nodes and elements. In particular, Model A was described with 381,306 elements and 905,526 nodes, and Model B featured 446,856 elements and 1,074,966 nodes. A convergence test for the mesh was performed by ensuring that a certain point was less than 10. This process validated the simulation results and showed that the mesh was not overly refined to describe model behavior at computational cost.

2.3. Material properties

This study used two material properties. Elastic modulus and Poisson's ratio (Table 1). The elastic modulus represents the material's stiffness; in other words, the material's resistance to deformation under stress. Poisson's ratio defines the ratio between transverse strain and axial strain when a load is applied. All materials were assigned as homogeneous, isotropic, and exhibiting linear elastic behavior.

2.4. Boundary condition and load application

To simulate the alveolar bone support, a boundary condition was used. This was obtained by holding the nodes on the base and side of the alveolar bone fixed in all three translational directions (x, y, and z axes = 0). In this way, the movement of the tooth was confined as though being rigidly supported by the jawbone.

Regarding the applied load, a vertical 600 N occlusal load was implemented to the occlusal surface of endocrown restorations using a rounded-end indenter made of stainless steel with a 6 mm diameter to apply a standardized tripod occlusal contact (Figure 2). The load was controlled with a crosshead speed of 0.5 mm/min. For this study, the von Mises stress theory was used to analyze the stress distribution across the tooth structures and restorations. This theory is a scalar representation derived from the stress tensor used to evaluate the yield point of materials subjected to complex loads.

The typical statistical tests used for FEA were not implemented due to the fact that FEA is utilized as a computer simulation instead of an experimental analysis. Each model's result was analyzed using the distribution of stress formed across each test model and thus assessed on the location of highest stress concentrations and compared via their stress patterns to each endocrown design tested.

3. Results

The finite element analysis (FEA) revealed distinct stress patterns among the models (Table 2, Figure 3). LDS restoration in Model A exhibited the highest VM stress value of (17.20) MPa, with stress concentrated at the occlusal loading area, whereas Model B displayed a broader stress distribution across the occlusal surface with a lower VM of (4.87) MPa. In Model B, the endocore showed a VM of (4.24) MPa, with stress localized at the occlusal and basal surfaces, and the cement layer between the endocore and veneering layer exhibited a VM of (3.92) MPa. The tooth-restoration cement layer in Model A exhibited slightly higher VM (5.16) MPa than in Model B (5.01) MPa, with stress more concentrated on the occlusal table in Model A.

The flowable composite in Model A displayed a VM of (1.63) MPa, with stresses more evident on the occlusal surface, compared to Model B with (1.33) MPa, where stresses were more uniformly distributed. In the enamel substrate, Model A demonstrated higher stress (16.05) MPa with concentration at the cervical rim, while Model B exhibited a lower VM of (9.88) MPa. Dentin stress was higher in Model A (4.37) MPa than in Model B (3.49) MPa, with stress in both models concentrated at the cervical region of the tooth.

4. Discussion

This study aimed to analyze the stress distribution across various endocrown restoration designs. The observational stress analysis revealed that the dual-layered design with Lava Ultimate endocore veneered with cemented LDS distributes the stresses more uniformly than a monolithic LDS endocrown restoration.

FEA has increasingly been popularized in dentistry for the use of predicting the biomechanical behavior of restorations while subjected to controlled load conditions (Zheng et al., 2021). An axial load was, in the current study, imposed with the aim of simulating the most frequent occlusal forces noted at the posterior site (Tribst et al., 2018). Posterior maximum occlusal forces have been noted to be higher than 580 N with mean forces of 522 N for males and 441 N for females (Bakke et al., 1992; Tortopidis et al., 1998). Given the fact that most of the occlusal forces noted at the molar area have an axial direction, an axial load of 600 N was, in the current study, imposed with the aim of mimicking the most extreme forces noted at the posterior segment (Dal Piva et al., 2018). Both models in the current work implemented the butt margin design. Al-Khafaji and Jasim (2020) noted endodontically prepared mandibular first premolars with an improved resistance to fracture when the butt margin design is implemented with reference to the shoulder design.

The LDS CAD/CAM ceramic material (IPS e.max CAD), with an elastic modulus of 95 GPa and a flexural strength of 350

MPa, was selected as the control model. Recognized as one of the most popular restorative materials for crowns and endocrowns, IPS e.max CAD provides long-term clinical success and sufficient strength to withstand occlusal forces (Al-Dabbagh, 2021; Chen et al., 2021), along with adhesive properties, esthetic, and acceptable mechanical performance (Kwon et al., 2018). However, the computational analysis indicated that monolithic LDS endocrowns exhibited higher von Mises stress values at the occlusal contact area and cervical margin, with a peak stress of 17.20 MPa. Our results for Model A align with the findings of Tribst et al. (2018) and Zheng et al. (2021), who noted that the LDS with a high modulus of elasticity contributes in stress to be accumulated in critical regions, restricting stress distribution to a wider region of the surrounding tooth structure, likely due to the significant elastic mismatch within the tooth-restoration complex. This is particularly relevant given that the biomechanical performance of restorative materials is directly influenced by their elastic modulus and thickness relative to the applied axial load, as Gresnigt et al. (2016) reported. A material with a high elastic modulus, such as LDS, lacks the flexibility to absorb occlusal forces, resulting in stress accumulation that may contribute to catastrophic fractures extending into the tooth structure, compromising restoration longevity and reparability (Sedrez-Porto et al., 2020; El Ghoul et al., 2019). Dental restorations' longevity depends on their ability to effectively distribute occlusal stresses and minimize stress concentrations that could lead to material fatigue or failure (He et al., 2021). One of the most critical factors influencing the longevity of dental restorations is their ability to resist crack initiation and propagation under cyclic occlusal forces (Rocca et al., 2018). Excessive stress accumulation at specific regions, such as the cervical margin or occlusal loading sites, can create microfractures that propagate over time, leading to catastrophic failure (Rocca et al., 2018; Kim et al., 2021).

Conversely, the dual-layered design demonstrated the ability to replicate the biomechanical behavior of natural teeth, leading to more favorable stress distribution patterns. The findings were consistent with Shams et al. (2022); in their study, the dual-layered endocrown significantly improved the biomechanical performance for premolar teeth. These results emphasize the significance of closely mimicking the properties of natural tooth substrates to enhance restorative performance (Attik et al., 2024; Madeira et al., 2024). Lava Ultimate, employed as the endocore material, consists of a composite resin microstructure enhanced with silica-zirconia nanoparticles (silica: 20 nm; zirconia: 4–11 nm) and nanoparticle clusters ranging from 0.6 to 10 µm. This material has an elastic modulus of 12.5 MPa, comparable to dentin at 18.1 MPa (Belli et al., 2017). It exhibits greater resiliency compared to lithium disilicate materials, allowing it to absorb forces effectively with mechanical properties closely resembling those of natural teeth, as supported by previous studies (Madeira et al., 2024; Ural & Çağlayan, 2021; Zheng et al., 2021). The resulting elastic gradient enables the LDS veneering layer to dissipate stresses across the occlusal table, rather than concentrating them at the loading area and intaglio surface, thereby enhancing stress distribution and reducing the risk of localized failures. The limitations of this FEA study include assuming material properties as homogeneous and isotropic, which may not accurately represent the anisotropic behavior of dental tissues and materials. Furthermore, the loading conditions were limited to static, axial forces, which do not fully replicate the multidirectional and dynamic forces present in clinical conditions.

5. Conclusions

The findings of this study highlight the biomechanical advantage of dual-layered endocrown designs over monolithic LDS restorations. The dual-layered design demonstrated favorable stress distribution, reducing critical stress concentrations. These results suggest that dual-layered endocrowns may provide a more durable and effective restorative solution for endodontically treated teeth. Further experimental and clinical investigations are recommended to validate these computational findings and establish their practical implications in clinical dentistry.

Conflict of interest

The authors declare that there are no conflicts of interest regarding the publication of this manuscript.

Acknowledgments

The authors would like to thank Mustansiriyah University (www.uomustansiriyah.edu.iq), Baghdad, Iraq, for their support in the present work.

Funding: This study is part of MSc project and is partially self-funded.

References

1. Schestatsky R, Dartora G, Felberg R, Spazzin AO, Sarkis-Onofre R, Bacchi A, et al. Do endodontic retreatment techniques influence the fracture strength of endodontically treated teeth? A systematic review and meta-analysis. J Mech Behav Biomed Mater. 2019; 90:306-12.
2. Phang ZY, Quek SHQ, Teoh KH, Tan KBC, Tan K. A retrospective study on the success, survival, and incidence of complications of post-retained restorations in premolars supporting fixed dental prostheses with a mean of 7 years in function. Int J Prosthodont. 2020; 33:176-83.
3. Govare N, Contrepois M. Endocrowns: A systematic review. J Prosthet Dent. 2020; 123:411-8. e9.
4. Sedrez-Porto JA, da Rosa WLdO, Da Silva AF, Münchow EA, Pereira-Cenci T. Endocrown restorations: A systematic review and meta-analysis. J Dent. 2016; 52:8-14.
5. Pissis P. Fabrication of a metal-free ceramic restoration utilizing the monobloc technique. Pract Periodontics Aesthet Dent: PPAD. 1995; 7:83-94.
6. Biacchi G, Basting R. Comparison of fracture strength of endocrowns and glass fiber post-retained conventional crowns. Oper Dent. 2012; 37:130-6.
7. El-Damanhoury HM, Haj-Ali RN, Platt JA. Fracture resistance and microleakage of endocrowns utilizing three CAD-CAM blocks. Oper Dent. 2015; 40:201-10.
8. Chen Y, Yeung AW, Pow EH, Tsoi JK. Current status and research trends of lithium disilicate in dentistry: A bibliometric analysis. J Prosthet Dent. 2021; 126:512-22.
9. El Ghoul W, Özcan M, Silwadi M, Salameh Z. Fracture resistance and failure modes of endocrowns manufactured with different CAD/CAM materials under axial

and lateral loading. J Esthet Restor Dent. 2019; 31:378-87.
10. Sedrez-Porto JA, Münchow EA, Cenci MS, Pereira-Cenci T. Which materials would account for a better mechanical behavior for direct endocrown restorations? J Mech Behav Biomed Mater. 2020; 103:103592.
11. Tribst JPM, Dal Piva AMdO, Madruga CFL, Valera MC, Borges ALS, Bresciani E, et al. Endocrown restorations: Influence of dental remnant and restorative material on stress distribution. Dent Mater. 2018; 34:1466-73.
12. Huang M, Wang R, Thompson V, Rekow D, Soboyejo W. Bioinspired design of dental multilayers. J Mater Sci Mater Med. 2007; 18:57-64.
13. Jargalsaikhan U, Wan H, Leung N, Song X, Hu J, Su B, et al. Micromechanical modelling for bending behaviour of novel bioinspired alumina-based dental composites. Dent Mater. 2024; 40:1669-76.
14. Eskitaşçioğlu M, Küçük O, Eskitaşçioğlu G, Eraslan O, Belli S. The effect of different materials and techniques on stress distribution in CAD/CAM endocrowns. Strength Mater. 2020; 52:812-9.
15. Awada A, Nathanson D. Mechanical properties of resin-ceramic CAD/CAM restorative materials. J Prosthet Dent. 2015; 114:587-93.
16. Della Bona A, Corazza PH, Zhang Y. Characterization of a polymer-infiltrated ceramic-network material. Dent Mater. 2014; 30:564-9.
17. Fathy H, Hamama HH, El-Wassefy N, Mahmoud SH. Clinical performance of resin-matrix ceramic partial coverage restorations: a systematic review. Clin Oral Investig. 2022; 26:3807-22.
18. Goujat A, Abouelleil H, Colon P, Jeannin C, Pradelle N, Seux D, et al. Mechanical properties and internal fit of 4 CAD-CAM block materials. J Prosthet Dent. 2018; 119:384-9.
19. Ural Ç, Çağlayan E. A 3-dimensional finite element and in vitro analysis of endocrown restorations fabricated with different preparation designs and various restorative materials. J Prosthet Dent. 2021; 126:586. e1-. e9.
20. Albelasy EH, Hamama HH, Tsoi JK, Mahmoud SH. Fracture resistance of CAD/CAM occlusal veneers: a systematic review of laboratory studies. J Mech Behav Biomed Mater. 2020; 110:103948.
21. Shams A, Elsherbini M, Elsherbiny AA, Özcan M, Sakrana AA. Rehabilitation of severely-destructed endodontically treated premolar teeth with novel endocrown system: biomechanical behavior assessment through 3D finite element and in vitro analyses. J Mech Behav Biomed Mater. 2022; 126:105031.
22. Dartora G, Pereira GKR, de Carvalho RV, Zucuni CP, Valandro LF, Cesar PF, et al. Comparison of endocrowns made of lithium disilicate glass-ceramic or polymer-infiltrated ceramic networks and direct composite resin restorations: fatigue performance and stress distribution. J Mech Behav Biomed Mater. 2019; 100:103401.
23. Zhu J, Rong Q, Wang X, Gao X. Influence of remaining tooth structure and restorative material type on stress distribution in endodontically treated maxillary premolars: A finite element analysis. J Prosthet Dent. 2017; 117:646-55.

24. Zheng Z, He Y, Ruan W, Ling Z, Zheng C, Gai Y, et al. Biomechanical behavior of endocrown restorations with different CAD-CAM materials: A 3D finite element and in vitro analysis. J Prosthet Dent. 2021; 125:890-9.
25. Gresnigt MM, Özcan M, van den Houten ML, Schipper L, Cune MS. Fracture strength, failure type and Weibull characteristics of lithium disilicate and multiphase resin composite endocrowns under axial and lateral forces. Dent Mater. 2016; 32:607-14.
26. Bakke M, Michler L, Möller E. Occlusal control of mandibular elevator muscles. Eur J Oral Sci. 1992; 100:284-91.
27. Tortopidis D, Lyons M, Baxendale R, Gilmour W. The variability of bite force measurement between sessions, in different positions within the dental arch. J Oral Rehabil. 1998; 25:681-6.
28. [Dal Piva AMdO, Tribst JPM, Borges ALS, e Souza ROdA, Bottino MA. CAD-FEA modeling and analysis of different full crown monolithic restorations. Dent Mater. 2018; 34:1342-50.
29. Al-khafaji S, Jasim H. Fracture Resistance of Endodontically Treated Teeth Restored by Full Crown and Two Endocrowns Preparation Design Made from Lithium Disilicate Material (A Comparative in Vitro Study). Int Med J. 2020; 25:2531-42.
30. Al-Dabbagh RA. Survival and success of endocrowns: A systematic review and meta-analysis. J Prosthet Dent. 2021; 125:415. e1-. e9.
31. Kwon SJ, Lawson NC, McLaren EE, Nejat AH, Burgess JO. Comparison of the mechanical properties of translucent zirconia and lithium disilicate. J Prosthet Dent. 2018; 120:132-7.
32. Köseoğlu M, Furuncuoğlu F. Effect of polyetheretherketone and indirect composite resin thickness on stress distribution in maxillary premolar teeth restored with endocrown: a 3D finite element analysis. J Biotechnol Strateg Health Res. 2020; 4:298-305.
33. Attik N, Richert R, Garoushi S. Biomechanics, Bioactive and Biomimetic Philosophy in Restorative Dentistry‒Quo vadis? J Dent. 2024:105036.
34. Madeira L, Weber KR, Carpenedo N, Zhang Y, Porto TS, Meira JBC, et al. Effect of elastic gradients on the fracture resistance of tri-layer restorative systems. Dent Mater. 2024.
35. Habelitz S, Marshall S, Marshall Jr G, Balooch M. Mechanical properties of human dental enamel on the nanometre scale. Arch Oral Biol. 2001; 46:173-83.
36. Craig RG, Peyton FA. Elastic and mechanical properties of human dentin. J Dent Res. 1958; 37:710-8.
37. Reinhardt RA, Krejci R, Pao Y, Stannard J. Dentin stresses in post-reconstructed teeth with diminishing bone support. J Dent Res. 1983; 62:1002-8.
38. Rocca GT, Daher R, Saratti CM, Sedlacek R, Suchy T, Feilzer AJ, et al. Restoration of severely damaged endodontically treated premolars: The influence of the endo-core length on marginal integrity and fatigue resistance of lithium disilicate CAD-CAM ceramic endocrowns. J Dent. 2018; 68:41-50.
39. Kim SY, Kim BS, Kim H, Cho SY. Occlusal stress distribution and remaining crack propagation of a cracked tooth treated with different materials and designs: 3D finite element analysis. Dent Mater. 2021; 37:731-40.

40. Tribst JPM, Dal Piva AM, de Melo RM, Borges AL, Bottino MA, Özcan M. Influence of restorative material and cement on the stress distribution of posterior resin-bonded fixed dental prostheses: 3D finite element analysis. J Mech Behav Biomed Mater. 2019; 96, 279-284.
41. Soares CJ, Soares PV, Santos-Filho PCF, Castro CG, Magalhaes D, Versluis A. The influence of cavity design and glass fiber posts on biomechanical behavior of endodontically treated premolars. J Endod. 2008; 34:1015-9.
42. Aversa R, Apicella D, Perillo L, Sorrentino R, Zarone F, Ferrari M, et al. Non-linear elastic three-dimensional finite element analysis on the effect of endocrown material rigidity on alveolar bone remodeling process. Dent Mater. 2009; 25:678-90.
43. Yamaguchi S, Kani R, Kawakami K, Tsuji M, Inoue S, Lee C, et al. Fatigue behavior and crack initiation of CAD/CAM resin composite molar crowns. Dent Mater. 2018; 34:1578-84.
44. He J, Zheng Z, Wu M, Zheng C, Zeng Y, Yan W, et al. Influence of restorative material and cement on the stress distribution of endocrowns: 3D finite element analysis. BMC Oral Health. 2021; 21:1-9.

Table 1: Elastic modulus and Poisson's ratio

Structure (tissue/material)	Elastic modulus (GPa)	Poisson's ratio	Reference
Enamel	84.1	0.33	(Habelitz et al., 2001)
Dentine	18.6	0.31	(Craig & Peyton, 1958)
Lava Ultimate	12.77	0.3	(Madeira et al., 2024)
IPS E.max	95	0.22	(Madeira et al., 2024)
Gutta percha	0.00069	0.45	(Reinhardt et al., 1983)
Flowable composite	7	0.25	(Zheng et al., 2021)
Resin Cement	8.3	0.24	(Tribst et al., 2019)
Periodontal ligament	0.05	0.45	(Soares et al., 2008)
Cortical bone	10.7	0.30	(Aversa et al., 2009)
Cancellous bone	0.91	0.30	(Aversa et al., 2009)
Stainless steel indenter	210	0.3	(Yamaguchi et al., 2018)

Table 2: Maximum von Mises stress values (MPa) in different parts of the models

Structure (tissue/material)	Model A	Model B
Enamel	16.05	9.88
Dentine	4.37	3.49
IPS e.max CAD	17.20	4.87
Lava Ultimate	-	4.24
Cement 1	5.16	5.01
Cement 2	-	3.92
Flowable composite	1.63	1.33
Gutta percha	0.00026	0.000141

Figure 1: Labeled illustration of Monolithic LDS Endocrown (A) and Dual-Layered Endocrown (B)**.**

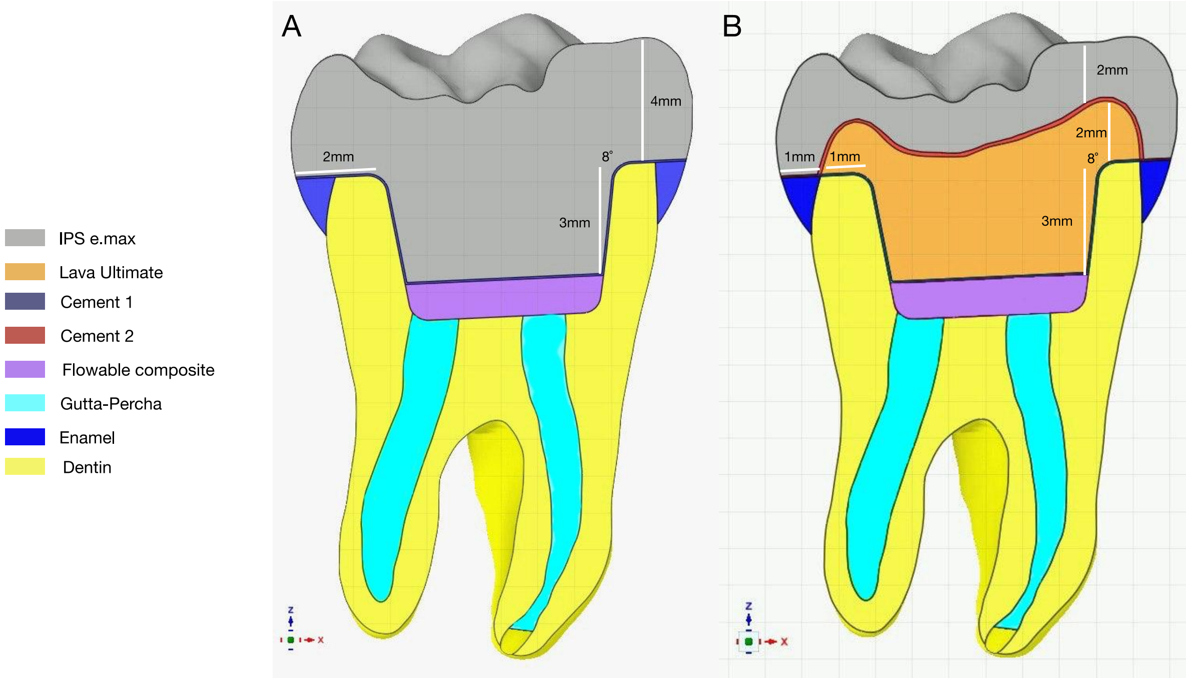

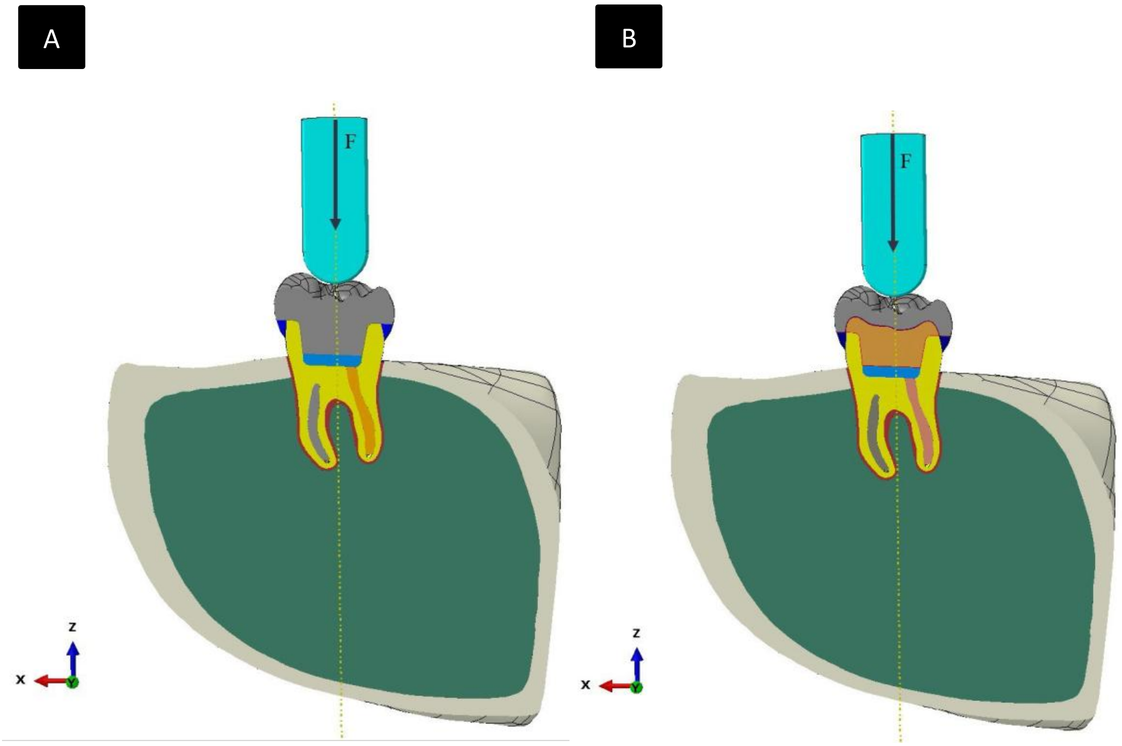

Figure 2: FEA Model for Endocrown Testing: Cross section of mandibular molar model with endocrown restoration systems under a 6 mm indenter applying tripod contact. A: Model A (Monolithic endocrown), B: Model B (Dual-layered endocrown).

Model A (Monolithic)	**Model B (Dual Layered)**

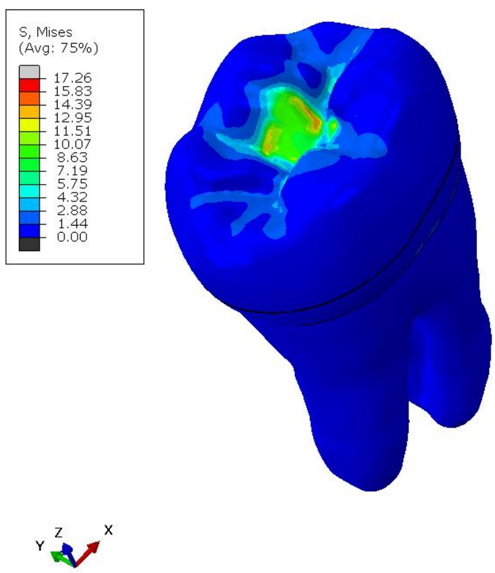

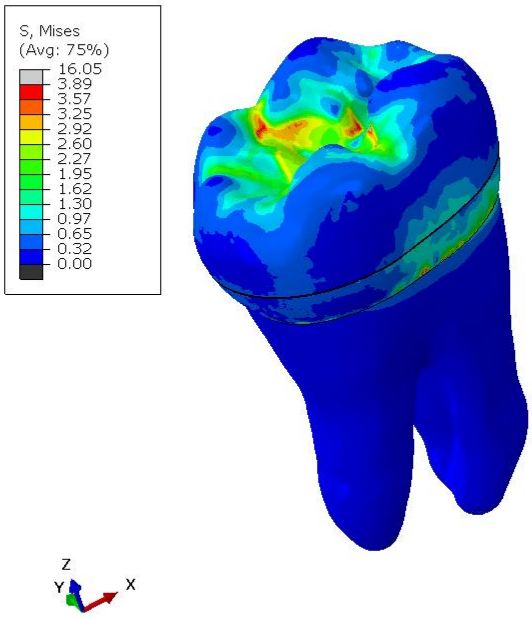

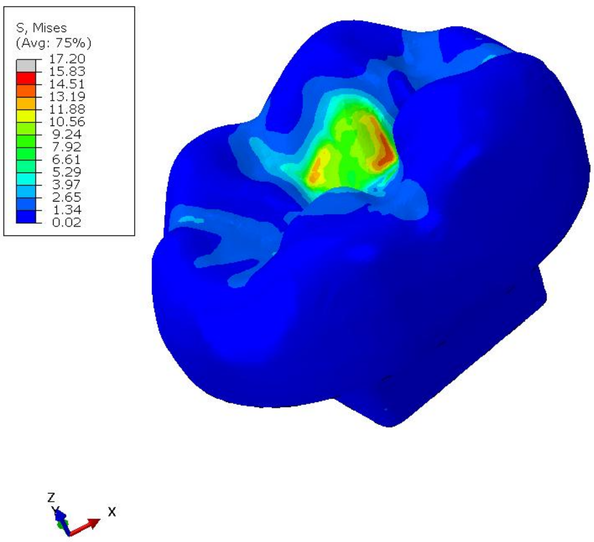

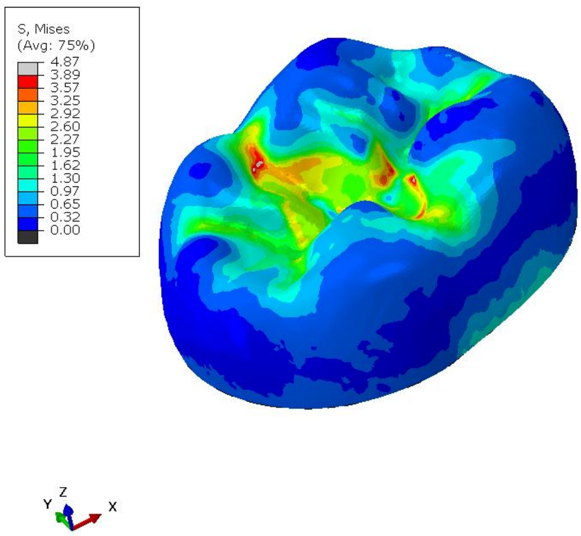

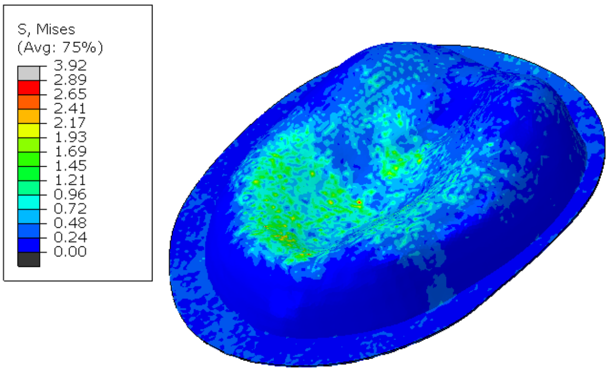
S, Mises
(Avg: 75%)
3.92
2.89
2.65
2.41
2.17
1.93
1.69
1.45
1.21
0.96
0.72
0.48
0.24
0.00

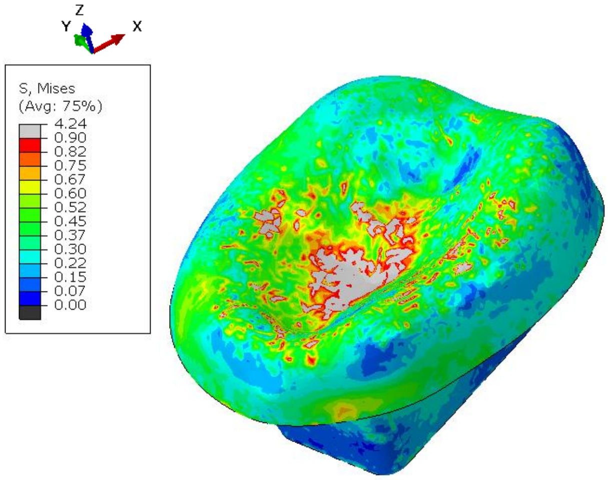
Z
Y
X
S, Mises
(Avg: 75%)
4.24
0.90
0.82
0.75
0.67
0.60
0.52
0.45
0.37
0.30
0.22
0.15
0.07
0.00

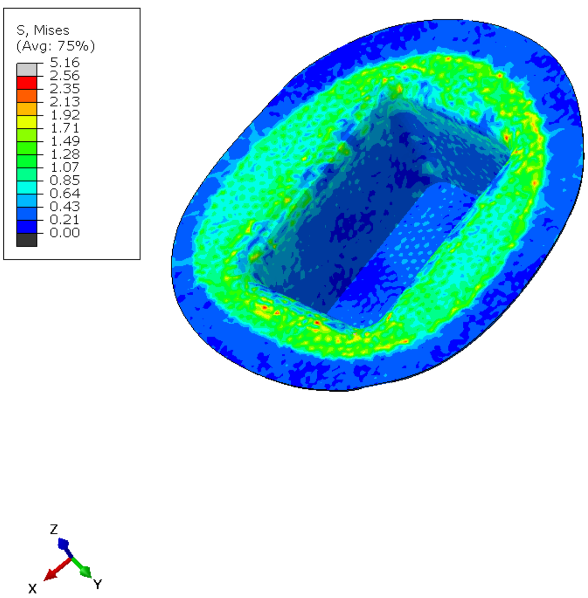
S, Mises
(Avg: 75%)
5.16
2.56
2.35
2.13
1.92
1.71
1.49
1.28
1.07
0.85
0.64
0.43
0.21
0.00
Z
X
Y

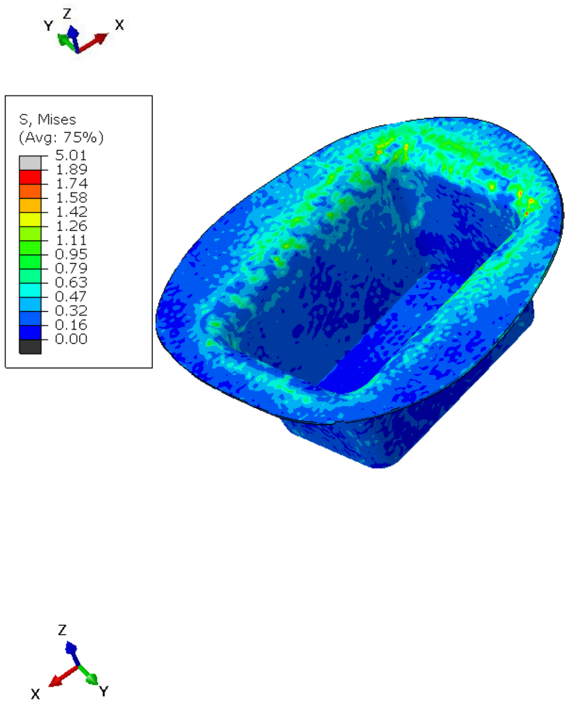
Z
Y
X
S, Mises
(Avg: 75%)
5.01
1.89
1.74
1.58
1.42
1.26
1.11
0.95
0.79
0.63
0.47
0.32
0.16
0.00
Z
X
Y

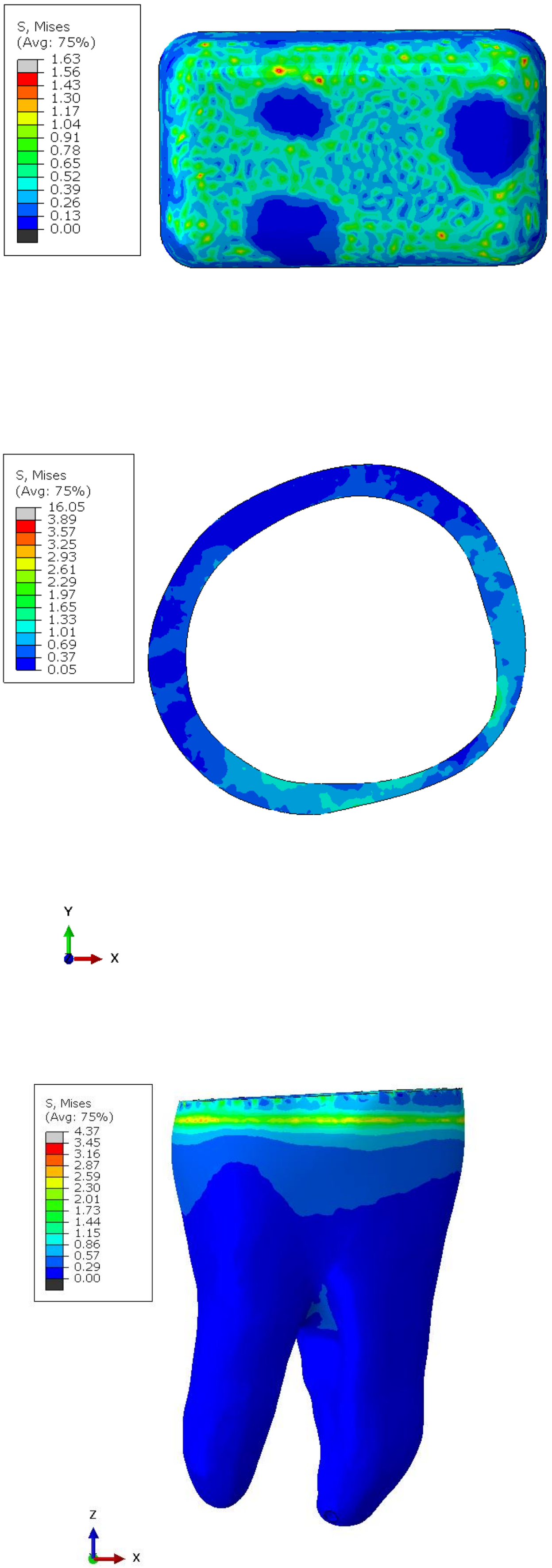
S, Mises
(Avg: 75%)
1.63
1.56
1.43
1.30
1.17
1.04
0.91
0.78
0.65
0.52
0.39
0.26
0.13
0.00
S, Mises
(Avg: 75%)
16.05
3.89
3.57
3.25
2.93
2.61
2.29
1.97
1.65
1.33
1.01
0.69
0.37
0.05
Y
X
S, Mises
(Avg: 75%)
4.37
3.45
3.16
2.87
2.59
2.30
2.01
1.73
1.44
1.15
0.86
0.57
0.29
0.00
Z
X

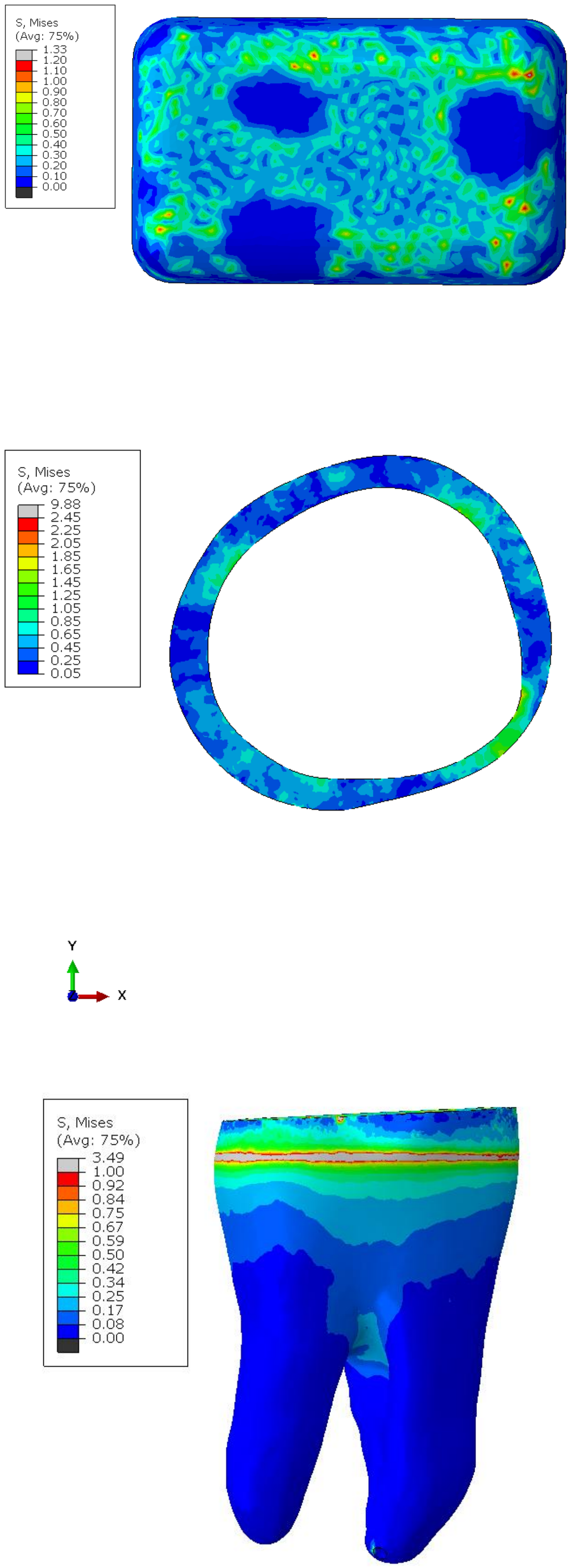
S, Mises
(Avg: 75%)
1.33
1.20
1.10
1.00
0.90
0.80
0.70
0.60
0.50
0.40
0.30
0.20
0.10
0.00
S, Mises
(Avg: 75%)
9.88
2.45
2.25
2.05
1.85
1.65
1.45
1.25
1.05
0.85
0.65
0.45
0.25
0.05
Y
X
S, Mises
(Avg: 75%)
3.49
1.00
0.92
0.84
0.75
0.67
0.59
0.50
0.42
0.34
0.25
0.17
0.08
0.00

Figure 3: Von Mises Stress Distribution: Stress distribution across the enamel, dentin, endocrown restoration, and surrounding structures, highlighting areas of high-stress concentration. Left: Model A (Monolithic LDS Endocrown), Right: Model B (Dual-layered endocrown restoration using Lava Ultimate endocore)